American Mineralogist, Volume 83, pages 159–166, 1998

Structural variations induced by thermal treatment in lead feldspar ($PbAl_2Si_2O_8$)

MARIO TRIBAUDINO,[1] PIERA BENNA,[1,2] AND EMILIANO BRUNO[1,2]

[1] Dipartimento di Scienze Mineralogiche e Petrologiche, Via Valperga Caluso 35, I-10125 Torino, Italy
[2] Centro di Studi sulla Geodinamica delle Catene Collisionali (C.N.R.), Via Accademia delle Scienze 5, I-10123 Torino, Italy

ABSTRACT

Lead feldspar single crystals were annealed at T = 1050 and 1000 °C, starting from a disordered metastable configuration (PbF_H, Q_{od} = 0) and from an ordered configuration (PbF_L, Q_{od} = 0.89). Single-crystal data collection and refinement in space group $I2/c$ show that the degree of Al-Si order increases to Q_{od} = 0.42 after annealing the disordered PbF_H at 1050 °C and decreases to Q_{od} = 0.70 after annealing the ordered PbF_L sample at 1000 °C. This suggests that the equilibrium Q_{od} is between 0.70 and 0.42 for temperatures between 1000 and 1050 °C, where anorthite or strontium feldspar are almost completely ordered. A residual in the difference-Fourier map because of positional disorder was observed near the Pb site in all the refined crystals. The average y/b_{Pb} coordinate changes with increasing Al-Si disorder, as Pb approaches the glide plane. A significant decrease in the intensity of b-type reflections was consequently observed. A spontaneous strain, with the main axis almost parallel to the a axis, is associated with Al-Si ordering. Pb polyhedral deformation related with Q_{od} accounts for the observed strain. A calibrating equation, $Q_{od} = [(8.427(2) - a) / 0.048(3)]^{1/2}$, has been calculated and applied to the unit-cell parameters obtained from subsequent thermal treatments and from Bruno and Facchinelli (1972) to define the evolution of the Q_{od} vs. the treatment temperature. The thermal behavior of the Q_{od} could then be bracketed, suggesting T_c between 1150 and 1200 °C for the $I2/c$-$C2/m$ phase transition induced by the Al-Si order-disorder process.

INTRODUCTION

Al-Si ordering in feldspars and the effects of substituting different non-tetrahedral cations have been a subject of research over many years (Ribbe 1994 and references therein). For feldspars with an Al:Si ratio of 1:1, the interest focussed initially on anorthite. Almost no disorder was detected between sites occupied by Al and Si in natural samples (Megaw et al. 1962; Wainwright and Starkey 1971; Kalus 1978). According to the Al-avoidance rule, formation of Al-O-Al linkages and hence Al-Si disorder is energetically unfavorable in feldspars with an Al:Si ratio of 1:1. However subsequent observations in anorthite heated close to the melting point show that some Al-Si disorder (Q_{od} = 0.78 at T = 1530 °C; Bruno et al. 1976) is present and is an equilibrium feature (Benna et al. 1985). Recently, thermodynamic behavior (Carpenter 1992) and kinetics of ordering in anorthite (Carpenter 1991a, 1991b; Salje et al. 1993) were described using Landau theory.

Recent investigations have focussed on feldspars with non-tetrahedral cations other than Ca, such as Sr or Pb. Structural, microtextural, and spectroscopic evolution of Al-Si order has been monitored in strontium feldspar (SrF) (Benna et al. 1995). In particular, metastable disorder was observed after short annealing of SrF samples synthesized from melt. Samples annealed for longer times and assumed to have achieved a close approach to equilibrium showed degrees of order, Q_{od}, which deviated significantly from complete order. For lead feldspar (PbF), Bruno and Facchinelli (1972) determined the unit-cell parameters for samples with different annealing histories. Significant changes in cell parameters were related to changes in the degree of Al-Si order. Although no calibration was given by the authors, a significant spontaneous strain associated with Al-Si ordering is present in lead feldspar. Recently, the structures of ordered ($I2/c$) and disordered ($C2/m$) lead feldspar have been determined (Benna et al. 1996). Disordered lead feldspar has a "split Pb-site configuration," whereas the ordered structure has the Pb atom displaced further from the c glide plane than Ba or Sr in barium and strontium feldspars. In addition, PbF samples that have been hydrothermally treated show strong b-type superstructure reflections and sharp IR absorption bands, but after thermal treatment at higher temperatures ($T \approx$ 1000 °C), the b-type reflections disappear and the linewidth of IR peaks increases (Bruno and Facchinelli 1972). It appears that significant Al-Si disorder can be achieved in lead feldspar by heating at temperatures lower than those required to disorder Al and Si in calcium and strontium feldspars. In this paper the structures of lead feldspars with intermediate degree of order are described.

0003–004X/98/0102–0159$05.00

TABLE 1. Single-crystal data for lead feldspars (standard deviations in parentheses)

Crystal	PbF_L1h	PbF_L16h	PbF_L64h	PbF_H136h
a (Å)	8.395(1)	8.399(2)	8.405(1)	8.418(2)
b (Å)	13.081(3)	13.061(4)	13.063(3)	13.076(4)
c (Å)	14.343(2)	14.334(3)	14.344(2)	14.365(4)
β (°)	115.27(1)	115.28(1)	115.29(1)	115.28(1)
V (Å^3)	1424.3	1421.8	1423.9	1429.8
μ (mm^{-1})	24.29	24.33	24.29	24.19
Crystal size (mm)	0.14 × 0.09 × 0.03	0.14 × 0.09 × 0.03	0.14 × 0.09 × 0.03	0.13 × 0.10 × 0.03
Refl. measured	7298	7310	7295	7328
Refl. observed $F_o \geq 4\sigma(F_o)$	2096	1311	1394	1443
Refl. b type	833	336	388	318
No. refl. b/No. refl. a	0.660	0.345	0.386	0.283
$\Sigma F^2_{o(b)}/\Sigma F^2_{o(a)}$ $F_o \geq 4\sigma(F_o)$	0.0994	0.0665	0.0660	0.0259
R	0.066	0.065	0.063	0.032
wR^2	0.160	0.118	0.148	0.063
Goodness of fit	1.12	1.12	0.94	0.92
No. of parameters	129	129	129	129

Note: $w = 1/[\sigma^2F_o^2 + (0.1P)^2]$, where $P = (F_o^2 + 2F_c^2)/3$. Space group is $I2/c$. Index ranges are $h \pm k \pm l$.

EXPERIMENTAL METHOD

The crystals used for data collection were obtained from isothermal annealing of PbF_L and PbF_H single crystals synthesized as in Benna et al. (1996). Ordered PbF_L was annealed at T = 1000 °C for 1, 16, and 64 h (samples PbF_L1h, PbF_L16h, and PbF_L64h, respectively); disordered PbF_H was annealed at T = 1050 °C for 136h (sample PbF_H136h). Data collection was performed with a Siemens P4 four-circle diffractometer, using graphite monochromatized Mo$K\alpha$ radiation (λ = 0.71073 Å), and the ϑ-2ϑ scan technique. Scan speeds are 1 to 15 °/min and 2θ ranged from 2 to 70°. Both a-type ($h + k = 2n$, $l = 2n$) and b-type ($h + k = 2n + 1$; $l = 2n + 1$) reflections were collected. In all samples b-type reflections were present with significant intensities. An empirical absorption correction based on the Ψ-scan method (North et al. 1968) was applied. The background and Lorentz polarization effect were corrected using the SHELXTL-PLUS 1990 System. Preliminary refinements were performed with the starting positions of PbF_L (Benna et al. 1996). However these refinements ended with non-positive definite values of displacement factors of many O atoms, high R values, and significant residuals in the difference-Fourier electron-density map, located in the proximity of the Pb site. The appearance of strong residuals near the Pb site in the difference-Fourier map is a common feature for Pb-bearing compounds (Moore et al. 1989, 1991; Szymanski 1988; Holtstam et al. 1995; Downs et al. 1995). A "split-atom model" with two sites, Pb′ and Pb″, was refined, with the Pb″ site at the position of the maximum residual density; the occupancy was fixed as 0.5 for both Pb′ and Pb″ and subsequently refined. The split model improved significantly the positional and displacement parameters of the lighter atoms and reduced the R value. Anisotropic refinement and correction for weight and isotropic extinction were performed at the end of the refinements. The position, occupancy, and displacement parameters of Pb′ and Pb″ are strongly correlated, and refinements with different combinations of the above parameters ended with similar R values. However the positions of lighter atoms were not significantly affected in the different split refinements. The split model can be regarded here simply as a method to give a better description of the Pb contribution. Final refinements with a single Pb site were done by fixing the parameters for T and O atoms to the positions obtained in the split refinements. This procedure obtained an average position for Pb that did not depend on the partitioning assumed for Pb′ and Pb″.

Unit-cell parameters, refinement data, atomic fractional coordinates, and displacement parameters are given in Tables 1 and 2. The degree of Al-Si order (Q_{od}) was calculated from average tetrahedral bond lengths as in Angel et al. (1990). Q_{od} values and the relevant bond lengths are reported in Tables 3[1] and 4[1]. In Figure 1 the Fourier maps near the Pb site are shown, for this work and the Benna et al. (1996) refinements. Significant changes in the Fourier map related to different Al-Si ordering are observed in the different samples. A tail is present and clearly increases with decreasing Q_{od}.

A few experiments were performed at varying annealing times to increase the previous data. The samples were annealed at temperatures between 900 and 1200 °C and then quenched in air (experimental conditions are reported in Table 5). A small loss in weight was observed with thermal treatment at T > 1100 °C. Microprobe analysis showed stoichiometric PbF crystals coexisting with a Pb-bearing glass, which forms as a consequence of the excess PbO in the starting materials (Benna et al. 1996). The stoichiometry of the lead feldspar was not observed to change after heating, whereas the Pb content significantly decreased in the glass. X-ray powder spectra were performed on these samples (Guinier camera, Cu$K\alpha$ radiation, λ = 1.54178 Å) and the relevant unit-cell parameters were obtained.

[1] For a copy of Tables 3 and 4, Document AM-98-004, contact the Business Office of the Mineralogical Society of America (see inside front cover of recent issue) for price information. Deposit items may also be available on the American Mineralogist web site (see inside back cover of a current issue for web address).

TABLE 2. Atomic fractional coordinates ($\times 10^4$), equivalent isotropic,* and anisotropic† displacement coefficients (Å^2 $\times$ 10^3) in lead feldspars

Site	x	y	z	U_{eq}	U_{11}	U_{22}	U_{33}	U_{12}	U_{13}	U_{23}
					PbF$_L$1h					
Pb	2716(1)	−96(1)	728(1)	28(0)	17(0)	44(0)	22(0)	−3(0)	8(0)	−2(0)
Pb′	2699(3)	−111(1)	736(1)	19(1)	13(1)	27(1)	15(1)	−7(0)	4(0)	−0(0)
Pb″	2758(6)	−29(5)	704(4)	61(2)	26(2)	119(5)	44(2)	9(2)	22(1)	−3(2)
$T_1(0)$	78(3)	1760(2)	1091(2)	11(0)	14(1)	14(1)	6(1)	−3(1)	6(1)	−1(1)
$T_1(z)$	22(4)	1797(2)	6164(2)	11(0)	13(1)	13(1)	9(1)	−3(1)	8(1)	−1(1)
$T_2(0)$	6948(4)	1201(2)	1711(2)	10(0)	13(1)	10(1)	8(1)	0(1)	7(1)	0(1)
$T_2(z)$	6873(4)	1140(2)	6749(2)	10(0)	12(1)	11(1)	9(1)	1(1)	7(1)	1(1)
$O_A(1)$	52(10)	1342(6)	9(5)	18(1)	27(4)	21(3)	9(2)	−2(2)	12(3)	−2(2)
$O_A(2)$	5944(10)	−5(4)	1459(6)	16(1)	15(3)	11(3)	22(3)	−2(2)	9(3)	0(2)
$O_B(0)$	8256(10)	1289(5)	1060(6)	17(1)	14(3)	19(3)	23(3)	−4(2)	12(3)	−1(2)
$O_B(z)$	8137(10)	1301(5)	6183(6)	20(1)	14(3)	22(3)	31(4)	−1(2)	17(3)	3(3)
$O_C(0)$	189(10)	2987(5)	1219(5)	18(1)	21(4)	17(3)	19(3)	−2(3)	10(3)	−2(2)
$O_C(z)$	190(10)	3108(5)	6323(6)	18(1)	18(3)	18(3)	20(3)	−3(2)	10(3)	−4(2)
$O_D(0)$	1845(11)	1233(6)	1957(5)	20(1)	21(4)	28(4)	11(3)	3(3)	8(3)	5(2)
$O_D(z)$	2021(10)	1210(5)	7011(5)	18(1)	18(3)	18(3)	15(3)	4(2)	4(3)	4(2)
					PbF$_L$16h					
Pb	2723(1)	−79(1)	719(1)	40(0)	17(0)	71(1)	28(0)	−10(1)	7(0)	−3(1)
Pb′	2731(3)	−136(3)	730(2)	24(1)	9(1)	39(1)	19(1)	−12(1)	3(1)	−0(1)
Pb″	2726(9)	58(12)	691(6)	66(3)	37(3)	109(6)	48(3)	31(3)	14(2)	−2(2)
$T_1(0)$	72(7)	1773(3)	1097(3)	11(1)	11(2)	13(2)	8(1)	−2(1)	4(1)	−2(1)
$T_1(z)$	25(8)	1793(3)	6153(3)	9(1)	13(4)	13(3)	4(2)	−3(2)	7(2)	0(2)
$T_2(0)$	6958(8)	1198(4)	1714(3)	8(1)	7(2)	8(2)	10(3)	4(2)	4(2)	1(1)
$T_2(z)$	6875(8)	1149(3)	6738(3)	10(1)	12(2)	11(2)	9(2)	−3(2)	6(2)	−2(1)
$O_A(1)$	20(24)	1345(7)	−10(10)	17(2)	22(4)	21(5)	11(3)	4(6)	9(3)	−3(4)
$O_A(2)$	5984(11)	−4(8)	1465(6)	16(2)	14(3)	15(4)	18(3)	−3(6)	6(3)	−5(4)
$O_B(0)$	8294(19)	1294(8)	1079(9)	21(3)	21(7)	21(6)	26(6)	−3(5)	15(6)	−5(4)
$O_B(z)$	8148(18)	1322(7)	6163(9)	19(3)	21(7)	15(5)	24(6)	−5(4)	11(5)	3(4)
$O_C(0)$	179(19)	3008(7)	1219(9)	20(3)	23(8)	11(5)	23(6)	−0(5)	8(6)	−1(4)
$O_C(z)$	200(17)	3105(7)	6325(9)	15(2)	12(6)	14(5)	20(5)	−1(4)	7(5)	−6(4)
$O_D(0)$	1837(19)	1244(8)	1963(9)	20(3)	20(7)	20(6)	14(5)	4(5)	0(5)	5(4)
$O_D(z)$	1986(18)	1228(8)	7021(9)	17(2)	15(6)	19(5)	16(5)	1(4)	6(5)	−1(4)
					PbF$_L$64h					
Pb	2723(1)	−76(1)	718(1)	41(0)	14(0)	74(1)	31(0)	−10(1)	6(0)	−5(1)
Pb′	2742(5)	5(6)	695(4)	63(2)	18(1)	118(4)	49(2)	13(2)	12(1)	1(2)
Pb″	2710(5)	−136(3)	737(3)	18(1)	10(1)	25(2)	15(1)	−15(1)	2(1)	−3(1)
$T_1(0)$	68(6)	1769(3)	1091(3)	9(1)	13(2)	8(1)	7(2)	−4(1)	7(2)	−1(1)
$T_1(z)$	27(6)	1799(3)	6162(3)	8(1)	8(2)	8(2)	7(2)	−3(1)	3(2)	−2(1)
$T_2(0)$	6968(6)	1195(3)	1720(3)	7(1)	6(2)	4(2)	11(3)	1(1)	2(2)	−1(1)
$T_2(z)$	6883(6)	1148(3)	6734(3)	8(1)	6(2)	8(2)	10(2)	−0(1)	5(2)	1(1)
$O_A(1)$	49(19)	1335(6)	3(10)	13(2)	22(4)	12(4)	8(3)	−1(4)	10(3)	0(4)
$O_A(2)$	5988(11)	−10(6)	1456(7)	14(2)	13(3)	5(4)	21(4)	3(4)	4(3)	9(4)
$O_B(0)$	8256(16)	1295(7)	1079(9)	19(3)	30(7)	13(4)	24(7)	−8(4)	20(6)	−2(4)
$O_B(z)$	8157(15)	1300(7)	6156(9)	20(2)	11(5)	20(5)	28(7)	−4(4)	8(5)	4(4)
$O_C(0)$	158(15)	3004(7)	1207(10)	18(2)	15(6)	19(5)	22(6)	−3(4)	10(5)	2(4)
$O_C(z)$	205(16)	3109(7)	6320(9)	16(2)	18(6)	17(5)	11(5)	−2(4)	4(5)	−5(3)
$O_D(0)$	1856(17)	1254(8)	1964(9)	20(3)	27(7)	23(5)	11(6)	2(4)	8(6)	7(4)
$O_D(z)$	1958(14)	1211(7)	7010(9)	16(2)	8(5)	21(5)	15(6)	−1(4)	0(5)	−3(4)
					PbF$_H$136h					
Pb	2723(1)	−45(1)	715(1)	50(0)	15(0)	98(1)	32(0)	−16(1)	6(0)	−5(1)
Pb′	2717(2)	−141(3)	743(2)	28(0)	13(0)	46(1)	23(0)	−11(0)	5(0)	5(0)
Pb″	2760(5)	171(8)	656(3)	46(1)	19(1)	72(3)	44(1)	14(1)	11(1)	20(1)
$T_1(0)$	55(3)	1775(1)	1105(2)	11(1)	9(1)	16(1)	8(1)	−4(1)	2(1)	1(1)
$T_1(z)$	40(4)	1794(1)	6147(2)	10(1)	11(2)	12(1)	10(2)	−3(1)	6(1)	−1(1)
$T_2(0)$	6942(4)	1186(2)	1719(2)	9(1)	6(1)	7(1)	12(2)	−1(1)	4(1)	−1(1)
$T_2(z)$	6897(4)	1153(1)	6735(2)	10(1)	8(1)	12(1)	7(2)	−0(1)	2(1)	−1(1)
$O_A(1)$	21(13)	1342(3)	−10(7)	16(1)	19(2)	20(2)	12(1)	−1(3)	8(1)	−3(3)
$O_A(2)$	5992(4)	−3(4)	1462(3)	16(1)	10(1)	10(1)	25(2)	−1(2)	6(1)	−2(2)
$O_B(0)$	8219(10)	1311(4)	1084(6)	22(2)	17(4)	24(2)	27(5)	−4(2)	10(4)	1(2)
$O_B(z)$	8169(10)	1305(4)	6146(6)	22(2)	19(4)	22(2)	30(5)	−4(2)	14(4)	−1(2)
$O_C(0)$	160(10)	3025(4)	1233(6)	21(2)	23(4)	20(2)	21(4)	−6(2)	9(3)	3(2)
$O_C(z)$	206(9)	3092(3)	6310(6)	20(2)	14(3)	17(2)	27(4)	−6(2)	5(3)	−2(2)
$O_D(0)$	1876(10)	1242(4)	1980(6)	22(2)	18(4)	27(3)	15(4)	4(2)	2(4)	3(2)
$O_D(z)$	1946(10)	1222(4)	7007(6)	21(2)	16(4)	26(3)	16(4)	−2(2)	3(4)	−1(2)

Note: Pb = Non-split model. Pb′ = Split model with occupancies of 0.6. Pb″ = Split model with occupancies of 0.4.

* U_{eq} defined as one-third of the trace of the orthogonalized U_{ij} tensor.

† The anisotropic displacement exponent takes the form: $-2\pi^2(h^2a^{*2}U_{11} + k^2b^{*2}U_{22} + l^2c^{*2}U_{33} + 2hka^*b^*U_{12} + 2hla^*c^*U_{13} + 2klb^*c^*U_{23})$.

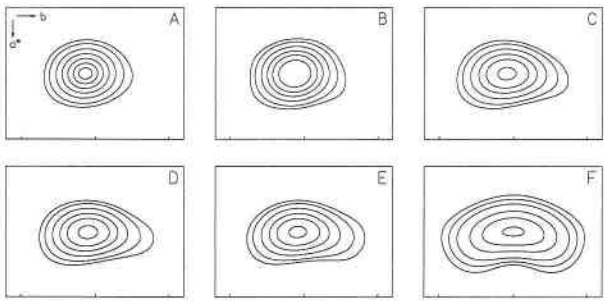

FIGURE 1. Electron-density maps for the Pb site viewed along the *c* axis; scale = 1 Å. (**A**) PbF_L (Benna et al. 1996). (**B**) PbF_L1h. (**C**) PbF_L16h. (**D**) PbF_L64h. (**E**) PbF_H136h. The contours drawn correspond to 20, 40, 80, 130, 180, and 240 $e^-Å^{-3}$. (**F**) PbF_H (Benna et al. 1996). The coordinates of the center of the plots are: $x = 0.27$, $y = 0$, $z = 0.07$ for A, B, C, D, E, and $z = 0.14$ for F.

TABLE 5. Experimental conditions and calculated Q_{od} values of lead feldspar with different annealing

Experiment number	Starting material	$T_{annealing}$ (°C)	P_{H_2O} (kbar)	*t* (h)	*a* (Å)	Q_{od} calc.
1 (PbF_H)	glass				8.428(1)	0
2 (PbF_L)	PbF_H	500	2.0	216	8.388(1)	0.90
3 (PbF_L1h)	PbF_L	1000		1	8.395(1)	0.82
4 (PbF_L16h)	PbF_L	1000		16	8.399(2)	0.76
5 (PbF_L64h)	PbF_L	1000		64	8.405(1)	0.68
6 (B&F)	gel	520	1.2	120	8.398(1)	0.78
7 (B&F)	6	1085		15	8.412(2)	0.56
8 (B&F)	7	1150		3	8.419(3)	0.41
9 (B&F)	glass	1150		12	8.416(2)	0.48
10 (B&F)	9	900		500	8.400(3)	0.75
11 (B&F)	10	520	1.2	120	8.395(1)	0.82
12 (PbF_H136h)	PbF_H	1050		136	8.418(2)	0.43
13	PbF_H	910		168	8.401(3)	0.74
14	11	900		3	8.399(1)	0.76
15	PbF_H	1050		238	8.413(3)	0.54
16	PbF_H	1200		16	8.428(2)	0
17	13	1200		2.25	8.432(1)	0

Note: 1, 2 = Benna et al. (1996); 3, 4, 5, 12, 13, 14, 15, 16, and 17 = this work; (B&F) = Bruno and Facchinelli (1972). The pressure is reported only for hydrothermal experiments.

RESULTS

Pb site and ordering

The above results show that the average position of the Pb atom moves away from the special position on the *m* plane in disordered *C*2/*m* lead feldspar (PbF_H, Benna et al. 1996) to the general position in ordered *I*2/*c* lead feldspar (PbF_L, Benna et al. 1996). The shift away from the plane can be monitored by changes in the *y*/*b* fractional coordinate for the average Pb site. The change of y/b_{Pb} is linear with Q_{od} (Fig. 2). Ordering and displacement from the glide plane are also related in strontium feldspar, at least for samples with $Q_{od} > 0.5$, but with much smaller shifts than in lead feldspar. Thus, displacement away from the glide plane depends strongly on the Al-Si distribution in the framework. Following the interpretation of Benna et al. (1996), the observed Pb configuration in disordered lead feldspar probably results from an average of local Pb structural configurations. Local Al-Si distributions have a pronounced effect on the lone-pair bearing cation, whose position is mostly sensitive to local charge imbalance. Local imbalance is expected in samples with disordered Al-Si distributions; a highly disordered framework induces a static Pb disorder and, in PbF_H, the Pb atom occupies a set of intermediate positions. In more ordered samples the Al-Si configuration around the Pb site is the same and the Pb atom occupies a single non-split position, situated well away from the mirror plane. This behavior is expected from the nature of the lone-pair bearing Pb cation, which frequently prefers an asymmetric coordination within the cavity (Moore et al. 1991 and references therein). Changes from disordered to ordered configurations are continuous and can be described by changes of the average *y*/*b* coordinate of Pb.

Unit-cell parameters, spontaneous strain, and ordering

Previous work has shown significant deviations of lead feldspar from trends of unit-cell parameters vs. volume or ionic radius (Bruno and Pentinghaus 1974; Ribbe 1994). The *b* of lead feldspar is slightly higher than that of barium feldspar, despite the ionic radius for Pb being close to that of Sr than Ba (ionic radii for eightfold-coordinated Sr, Pb, and Ba are, respectively, 1.26, 1.29, 1.42 Å; Shannon and Prewitt 1969). The descrepancy has been tentatively attributed to the lone pair (Ribbe 1994). However the anomalous behavior of *b* can be explained by considering the OA1-OA1 shared edge in common between Pb-centered polyhedra, through which Pb atoms are facing. The OA1-OA1 edge lies along the *b* axis,

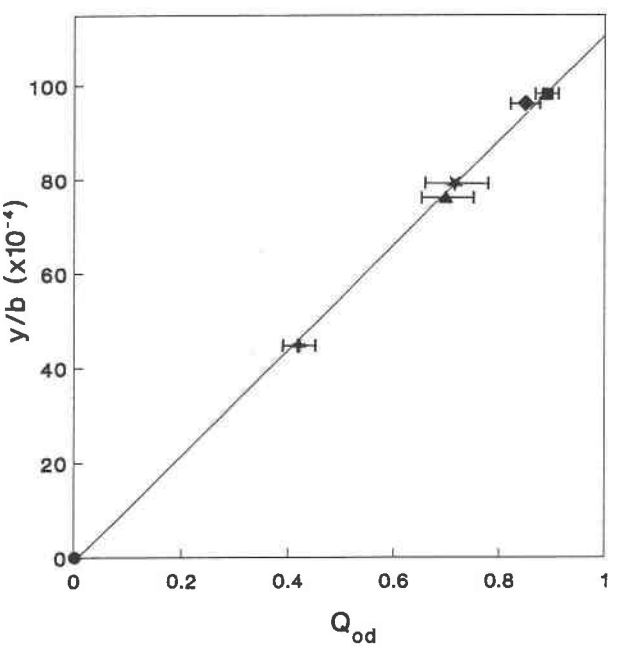

FIGURE 2. Absolute value of *y*/*b* fractional coordinate of the Pb site vs. Q_{od}. Circle and square = PbF_H and PbF_L, respectively (Benna et al. 1996); diamond = PbF_L1h; star: PbF_L16h; triangle = PbF_L64h; cross = PbF_H136h.

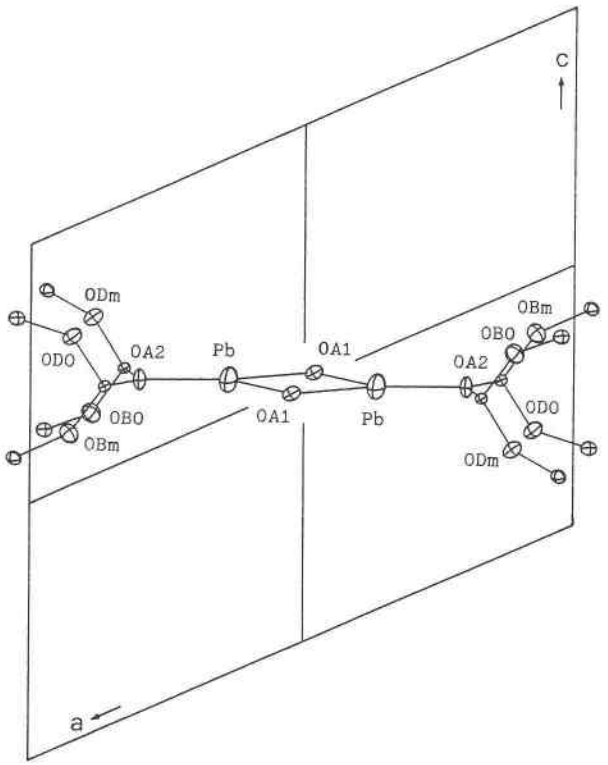

FIGURE 3. Partial projection on the (010) plane of PbF_H structure (e.g., *C2/m*, c = 7.174 Å) (Benna et al. 1996). The projection was slightly rotated to avoid overlapping of atoms. T atoms are not labeled.

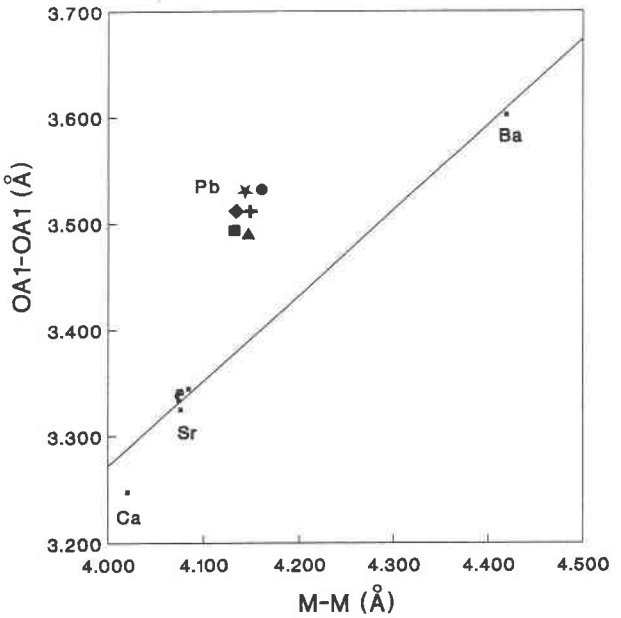

FIGURE 4. OA1-OA1 vs. M-M distances (see Fig. 3) in calcium feldspar (Wainwright and Starkey 1971), strontium feldspar (Chiari et al. 1975; Benna et al. 1995), lead feldspar (Benna et al. 1996; this work), and barium feldspar (Griffen and Ribbe 1976). Symbols as in Figure 2.

whereas the Pb-Pb distance is almost along a^* (Fig. 3). In Figure 4 the OA1-OA1 vs. M-M distances are plotted in calcium, strontium, lead, and barium feldspars. For reference the trend between strontium and barium feldspars has been drawn. The deviation from the trend is relatively small in anorthite, in spite of the different symmetry, but significant in lead feldspars; the OA1-OA1 distance is closer to the value of barium feldspar, whereas the Pb-Pb distance is closer to that found in strontium feldspars. The explanation is that a higher degree of relaxation occurs between OA1-OA1 pairs in lead feldspars, hence leading to a longer OA1-OA1 distance. An effect of the lone pair in Pb-bearing phases is to more tightly bond O atoms on one side of the cavity relative to O atoms on the other side. In lead feldspar the difference between the two Pb-OA1 distances is significantly greater. The shorter Pb-OA1 distance has a value that can be constrained along an ionic trend between Ba and Sr, whereas the other Pb-OA1 is significantly higher. As a consequence, greater relaxation along OA1-OA1 and a b value greater than from a merely ionic trend are observed.

Small changes, mainly in a, are related to the Al-Si ordering in lead feldspar (Fig. 5). A spontaneous strain was calculated on the samples refined in this work and on PbF_L (Benna et al. 1996), taking as reference state the completely disordered PbF_H sample (Benna et al. 1996) (Table 6). The strain ellipsoid has a cigar-like appearance, with the main axis (ϵ_1) almost along a (Fig. 6) and a deformation almost five times greater than along the other axes. This orientation with ordering is anomalous. In other feldspars a parameter changes with composition rather than with degree of Al-Si order. In lead feldspar, changes

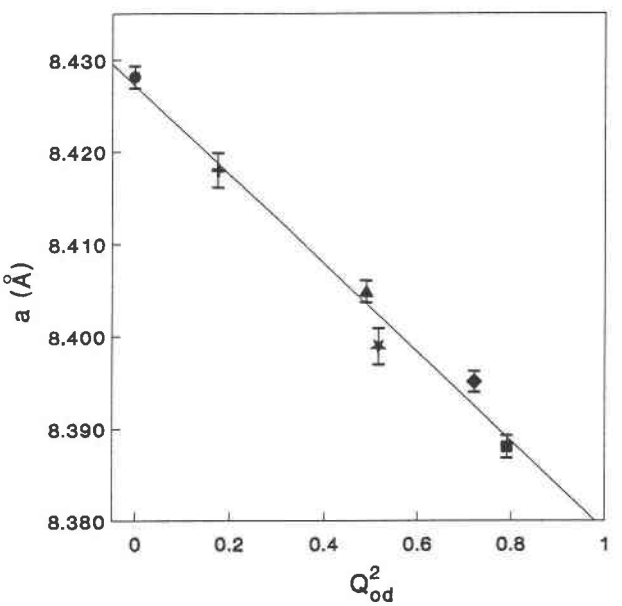

FIGURE 5. Value of the a unit-cell parameter vs. Q^2_{od}. Symbols as in Figure 2.

TABLE 6. Principal axes of the strain ellipsoids for lead feldspars

	Strain ($\times 10^{-3}$)	Angle with		
		a	*b*	*c*
		PbF_H136h—PbF_H		
ϵ_1	1.2(3)	4	90	111
ϵ_2	−1.5(3)	94	90	21
ϵ_3	−1.7(3)	90	0	90
		PbF_L64h—PbF_H		
ϵ_1	2.8(2)	6	90	109
ϵ_2	0.1(2)	96	90	19
ϵ_3	−0.7(3)	90	0	90
		PbF_L16h—PbF_H		
ϵ_1	3.5(3)	5	90	111
ϵ_2	0.7(3)	94	90	21
ϵ_3	−0.5(3)	90	0	90
		PbF_L1h—PbF_H		
ϵ_1	4.0(2)	6	90	110
ϵ_2	0.0(2)	96	90	20
ϵ_3	−2.1(3)	90	0	90
		PbF_L—PbF_H		
ϵ_1	4.8(2)	5	90	120
ϵ_2	0.4(2)	85	90	30
ϵ_3	−1.0(2)	90	0	90

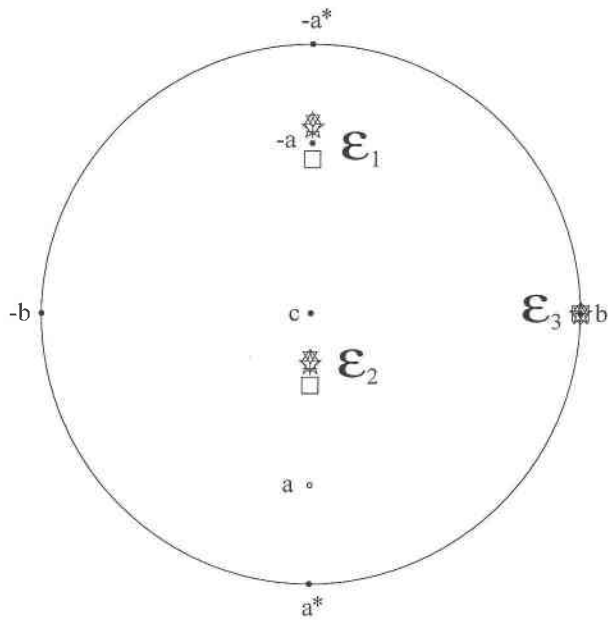

FIGURE 6. Stereographic projection showing the orientation of the principal axes, ϵ_1, ϵ_2, ϵ_3, of the spontaneous strain ellipsoids for the *C2/m-I2/c* transition in lead feldspar. ϵ_1 = main axis; a, b, c = real lattice vectors; a^* = reciprocal lattice vector. Symbols as in Figure 2.

in *a* with Q_{od} seem to be related to significant changes in the non-tetrahedral cation configuration. A geometrical explanation of this can be seen in a projection onto a plane normal to the *b* axis (Fig. 3). The Pb-Pb and Pb-OA2 distances, which both lie almost along a^*, increase significantly with disorder (respectively, from 4.132 to 4.189 Å and from 2.465 to 2.503 Å for PbF_L to PbF_H). The overall increase across the Pb polyhedra can be recognized in the OA2-OA2 distance, which increases from 9.042 to 9.193 Å. The deformation along a^* of the tetrahedral cage (from 6.139 to 6.045 Å) only partially compensates for the increase in OA2-OA2. The resulting effect is an increase of a^*; this effect together with small changes in the β angle account for the deformation along the *a* axis.

For a zone boundary *C2/m-I2/c* phase transition the relation between the scalar spontaneous strain and the order parameter is expected to be: $\epsilon_s \propto Q_{od}^2$. For lead feldspar, the strain comes mainly for changes in *a* because of the coupling between the position of the non-tetrahedral cation and the degree of Al-Si order. The expected relation $a \propto \epsilon_s \propto Q_{od}^2$ is observed (Fig. 5) and could be used to calibrate the degree of order. In strontium feldspar changes in Q_{od} from 0 to 0.86 do not significantly affect the Sr-Sr and Sr-OA2 distances (Benna et al. 1995), and the spontaneous strain with ordering is not significant.

The following equation was obtained by fitting the data (Fig. 5):

$$Q_{od} = \{[8.427(2) - a] / 0.048(3)\}^{1/2}$$

The thermal treatments here and in Bruno and Facchinelli (1972) are reported in Table 5, with relevant Q_{od} values calculated as above. The data in Table 5 refer to feldspars annealed from both disordered and ordered starting samples to bracket the equilibrium Q_{od} at the different temperatures. In Figure 7 the Q_{od} values vs. the annealing temperature are reported in anorthite and lead feldspar. For each of the annealing temperatures shown in Table 5 the arrows mark the longer treatments in lead feldspar. A marked decrease in Q_{od} between 800 and 1200 °C is observed in Figure 7. The transition to the disordered *C2/m* configuration is shown to occur between 1150 and 1200 °C (in anorthite a transition to the disordered $C\bar{1}$ configuration is predicted at 2010 °C, Carpenter 1992). The above data are not sufficient to constrain the thermodynamic behavior of the transition; however, comparison with equilibrium data on anorthite in Figure 7 (Benna et al. 1985; Carpenter 1992) shows that lead feldspar retains equilibrium configurations with highly disordered Al-Si in the subsolidus at significantly lower temperatures.

The *C2/m-I2/c* phase transition in lead feldspar

As discussed above, Al-Si ordering and the shift away from the mirror plane of the non-tetrahedral cation are related. Both contribute to the intensity of *b*-type reflections, which appear at the *C2/m-I2/c* phase transition. In the case when the non-tetrahedral cation is on the glide plane in an ordered sample, as in barium feldspar (Griffen and Ribbe 1976) the *I* lattice is simply due to Al-Si ordering. In strontium and lead feldspar both mechanisms contribute to the development of the *I* lattice. In theory, a completely disordered Al-Si configuration could still retain *I* lattice symmetry if the cation position is away from the plane, but this does not occur either in disor-

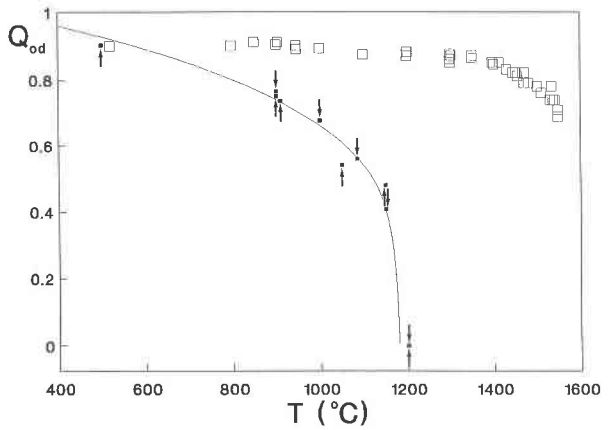

FIGURE 7. Thermal evolution of the Q_{od} in anorthite and in lead feldspar. Squares = anorthite (Benna et al. 1985; Carpenter 1992). Arrows = lead feldspar (Bruno and Facchinelli 1972; this work); for each T only samples with longer annealing (Table 5) are reported. Arrows up = experiments from more disordered starting materials; arrows down = experiments from more ordered starting materials. A best fit curve is shown to indicate the thermal evolution of the Q_{od} in lead feldspar.

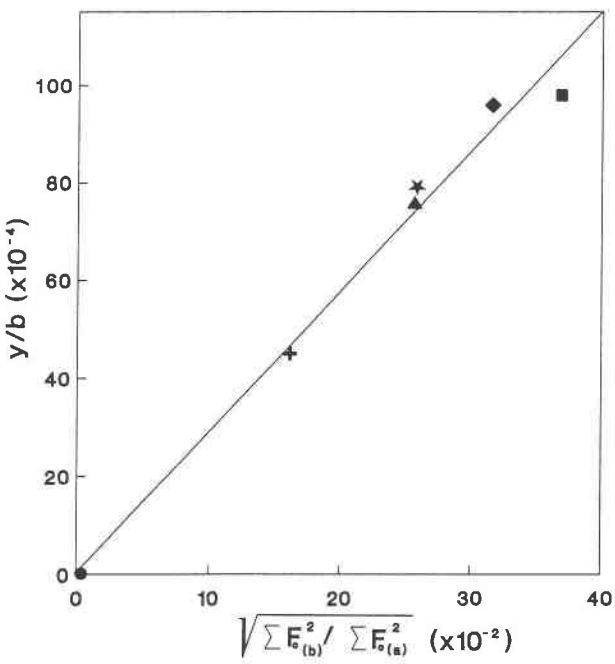

FIGURE 8. Absolute value of y/b coordinate of the Pb site vs. $\sqrt{\Sigma F^2_{o(b)}/\Sigma F^2_{o(a)}}$. Symbols as in Figure 2.

dered strontium or in lead feldspar. Complete Al-Si disorder increases the average symmetry of the framework, which forces the average cation position to the center of the polyhedron on the mirror plane. The deviation of the non-tetrahedral cation site from the *C2/m* symmetry can be expressed in terms of the length of the split vector 2 (y/b) b or, more simply, the fractional coordinate y/b of the non-tetrahedral cation. The b lattice parameter does not significantly change with Al-Si ordering in strontium and lead feldspars. As Q_{od} varies with $I^{1/2}$, where I is the intensity of a b-type reflection (Carpenter et al. 1990), relationships of the form $Q_{od} \propto I^{1/2} \propto 2\ (y/b)\ b \propto y/b$ are expected for strontium and lead feldspars.

In lead feldspar b-type reflections are much stronger than those in strontium feldspar for samples with the same degree of order. The sum of the intensities of b-type reflections relative to the sum of the intensities of a-type reflections ($\Sigma F^2_{o(b)}/\Sigma F^2_{o(a)}$) is 0.12 in ordered lead feldspar and 0.02 in strontium feldspar (Q_{od} = 0.89 and 0.86, respectively). The difference is because of the contribution of the non-tetrahedral cation. In lead feldspar the shift of the non-tetrahedral cation is much greater than in strontium feldspar (y/b_{Pb} = 0.010 and y/b_{Sr} = 0.002) and the total effect is enhanced by the higher scattering power of Pb in comparison with Sr. On the other hand, the contribution of the framework to the intensity of the b-type reflections is not expected to be significantly different in ordered lead and strontium feldspars. Simple calculation of the structure factors for a fictive structure with the framework coordinates as in PbF_L (Benna et al. 1996) and the Pb position fixed onto the glide plane shows that the value of $\Sigma F^2_{o(b)}/\Sigma F^2_{o(a)}$ decreases from 0.12 to 0.01. In lead feldspar the average fractional coordinate y/b_{Pb} clearly correlates with the square root of the intensity of b-type reflections (Fig. 8). The intensity of b-type reflections is therefore mainly due to the shift of the Pb atom.

The linear dependance y/b_{Pb} on Q_{od} (as seen in Fig. 2) suggests that, in lead feldspar, the displacement of Pb away from the plane can be considered directly related to Al-Si disorder. As with changes in tetrahedral bond lengths or spontaneous strain, the Pb displacement provides a parameter for determining Q_{od} that may be simpler to evaluate than directly measuring the Al-Si ordering itself.

Finally, the Al-Si ordering kinetics are significantly faster in lead feldspar than in alkaline-earth feldspars. For example, at T = 1000 °C, a sample with Q_{od} = 0.89 changed to Q_{od} = 0.70 after 64 h, whereas almost no change occurs in alkaline-earth feldspars under the same conditions. In view of the involvement of the Pb displacements, a catalytic effect of the Pb cation on Al-Si ordering is suggested. Further high temperature in situ and thermodynamic investigations are required to clarify the transition behavior.

ACKNOWLEDGMENTS

We thank Simon A.T. Redfern for critical reading and useful suggestions. Reviews from Ross J. Angel and Michael A. Carpenter greatly improved the manuscript. This work was supported by M.U.R.S.T.-Roma, C.S. Geodinamica Catene Collisionali CNR-Torino, and CNR-Roma.

REFERENCES CITED

Angel, R.J., Carpenter, M.A., and Finger, L.W. (1990) Structural variation associated with compositional variation and order-disorder behavior in anorthite-rich feldspars. American Mineralogist, 75, 150–162.

Benna, P., Zanini, G., and Bruno, E. (1985) Cell parameters of thermally treated anorthite. Al, Si configurations in the average structures of the

high temperature calcic plagioclases. Contributions to Mineralogy and Petrology, 90, 381–385.

Benna, P., Tribaudino, M., and Bruno, E. (1995) Al-Si ordering in Sr-feldspar $SrAl_2Si_2O_8$: IR, TEM and single-crystal XRD evidences. Physics and Chemistry of Minerals, 22, 343–350.

———(1996) The structure of ordered and disordered lead feldspar ($PbAl_2Si_2O_8$). American Mineralogist, 81, 1337–1343.

Bruno, E. and Facchinelli, A. (1972) Al,Si configurations in lead feldspar. Zeitschrift für Kristallographie, 136, 296–304.

Bruno, E. and Pentinghaus, H. (1974) Substitution of cations in natural and synthetic feldspars. In W.S. McKenzie and J. Zussman, Eds., The feldspars, p. 574–609. Manchester University Press, Manchester, U.K.

Bruno, E., Chiari, G., and Facchinelli, A. (1976) Anorthite quenched from 1530 °C: I. Structure refinement. Acta Crystallographica, B32, 3270–3280.

Carpenter, M.A. (1991a) Mechanisms and kinetics of Al-Si ordering in anorthite: I. Incommensurate structure and domain coarsening. American Mineralogist, 76, 1110–1119.

———(1991b) Mechanisms and kinetics of Al-Si ordering in anorthite: II. Energetics and a Ginzburg-Landau rate law. American Mineralogist, 76, 1120–1133.

———(1992) Equilibrium thermodynamics of Al/Si ordering in anorthite. Physics and Chemistry of Minerals, 19, 1–24.

Carpenter, M.A., Angel, R.J., and Finger, L.W. (1990) Calibration of Al/Si order variations in anorthite. Contributions to Mineralogy and Petrology, 104, 471–480.

Chiari, G., Calleri, M., Bruno, E., and Ribbe, P.H. (1975) The structure of partially disordered, synthetic strontium feldspar. American Mineralogist, 60, 111–119.

Downs, R.T., Hazen, R.M., Finger, L.W., and Gasparik, T. (1995) Crystal chemistry of lead aluminosilicate hollandite: A new high-pressure synthetic phase with octahedral Si. American Mineralogist, 80, 937–940.

Griffen, D.T. and Ribbe, P.H. (1976) Refinement of the crystal structure of celsian. American Mineralogist, 61, 414–418.

Holtstam, D., Norrestam, R., and Sjödin, A. (1995) Plumboferrite: New mineralogical data and atomic arrangement. American Mineralogist, 80, 1065–1072.

Kalus, C. (1978) Neue Strukturbestimmung des Anorthits under Berücksichtigung möglicher Alternativen. Inaugural-Dissertation, Universität München, Munich, Germany.

Megaw, H.D., Kempster, C.J.E., and Radoslovich, E.W. (1962) The structure of anorthite $CaAl_2Si_2O_8$: II. Description and discussion. Acta Crystallographica, 15, 1017–1035.

Moore, P.B., Sen Gupta, P.K., and Le Page, Y. (1989) Magnetoplumbite, $Pb^{2+}Fe^{3+}_{12}O_{19}$: Refinement and lone-pair splitting. American Mineralogist, 74, 1186–1194.

Moore, P.B., Sen Gupta, P.K., Shen, J., and Schlemper, E.O. (1991) The kentrolite-melanotekite series, $4Pb_2(Mn,Fe)^{3+}_2O_2[Si_2O_7]$: Chemical crystallographic relations, lone-pair splitting, and cation relation to $8URe_2$. American Mineralogist, 76, 1389–1399.

North, A.C.T., Phillips, D.C., and Mathews, F.S. (1968) A semi-empirical method of absorption correction. Acta Crystallographica, A24, 351–359.

Ribbe, P.H. (1994) The crystal structures of the aluminum-silicate feldspars. In I. Parsons, Ed., Feldspars and their reactions, p. 1–49. Kluwer Academic Publishers, Dordrecht.

Salje, E.K.H., Wruck, B., Graeme-Barber, A., and Carpenter, M.A. (1993) Experimental test of rate equations: Time evolution of Al-Si ordering in anorthite $CaAl_2Si_2O_8$. Journal of Physics: Condensed Matter, 5, 2961–2968.

Shannon, R.D. and Prewitt, C.T. (1969) Effective ionic radii in oxides and fluorides. Acta Crystallographica, B25, 925–945.

Szymanski, J.T. (1988) The crystal structure of beudantite, $Pb(Fe,Al)_3[(As,S)O_4]_2(OH)_6$. Canadian Mineralogist, 26, 923–932.

Wainwright, J.E. and Starkey, J. (1971) A refinement of the structure of anorthite. Zeitschrift für Kristallographie, 133, 75–84.

Manuscript received April 21, 1997
Manuscript accepted August 28, 1997